Surface dependency in thermodynamics of ideal gases

Altug Sisman[1]

Energy Institute, Istanbul Technical University, 80626-Maslak, Istanbul, Turkey
and
Institute of Thermodynamics, Technical University of Berlin, 10623 Berlin, Germany

E-mail: sisman@thermodynamik.tu-berlin.de and sismanal@itu.edu.tr

Abstract
The Casimir-like size effect rises in ideal gases confined in a finite domain due to the wave character of atoms. By considering this effect, thermodynamic properties of an ideal gas confined in spherical and cylindrical geometries are derived and compared with those in rectangular geometry. It is seen that an ideal gas exhibits an unavoidable quantum surface free energy and surface over volume ratio becomes a control variable on thermodynamic state functions in microscale. Thermodynamics turns into non-extensive thermodynamics and geometry difference becomes a driving force since the surface over volume ratio depends on the geometry.

PACS numbers: 05.70.−a, 05.90.+m, 51.30.+i

1. Introduction

In any stationary wave field a bounded domain exhibits Casimir-like size effects as long as the maximum wavelength is bigger than the size of the domain. The original Casimir effect is an attractive interaction between two parallel conducting neutral plates at absolute zero temperature due to the alteration of the zero point electromagnetic wave field between the conducting boundaries [1]. In general, the effect depends on temperature, geometric and electromagnetic properties of the boundary material and it can be repulsive under some geometrical conditions [2–4]. The effect becomes important on micron and sub-micron scales. Recent developments in nanotechnology make it possible to produce some devices on nanoscale [5, 6]. Therefore, the applications of the Casimir effect in technology have become a current issue [7–13]. The number of studies on the thermodynamics of the Casimir effect have been increasingly [14–20].

---

[1] Now at Technical University of Berlin.

An equivalent effect has been observed in an acoustic wave field [21]. In a recent study, another equivalent effect has been theoretically proposed and examined by considering the wave character of atoms in ideal gases confined in a rectangular box [22]. For rectangular geometry, it has been shown that the Casimir-like size effects in ideal gases cause size-dependent additional terms in the thermodynamic state functions like the free energy. Some consequences of this size dependence are anisotropic pressure, diffusion due to the size difference and thermosize effects similar to thermoelectric effects [22]. In the present study, spherical and cylindrical confinement geometries are considered and it is shown that an ideal gas confined in a finite domain exhibits an unavoidable quantum surface free energy, F_A, which depends on the surface over volume ratio of the domain, A/V, besides the number of particles and temperature. This surface energy is also proportional to the most probable de Broglie wavelength of the particles, which depends on temperature and molecular mass. Therefore, it is a consequence of the wave character of the particles and it is called 'quantum surface free energy'. While the classical surface energy results from the interactions between the particles, the quantum surface energy arises from the surface modes. Unavoidable existence of F_A makes the thermodynamics non-extensive, surface and size dependent (namely A/V) in general on account of the wave character of atoms. Deviations from ordinary thermodynamics should become noticeable on the micron and sub-micron scale. Apart from their relevance to fundamental and non-extensive thermodynamics the results may affect the phenomena in nano and microstructures.

2. Thermodynamic properties of a monatomic ideal gas confined in a spherical geometry

2.1. Single-particle partition function

The solution of the Schrödinger equation for a single-particle confined in a spherical vessel gives the following translational energy eigenvalues of the form

$$\varepsilon_{nlm} = \frac{\hbar^2}{2m_a R^2} x_{nl}^2 \qquad \text{with} \quad n = 1, 2, 3, \ldots; \quad l = 0, 1, 2, 3, \ldots \qquad \text{and}$$
$$m = -l, \ldots, -1, 0, 1, \ldots, l, \tag{1}$$

where $\hbar$ is the reduced Planck constant, m_a is the atomic mass, R is the radius of spherical vessel and x_{nl} is the nth root of the spherical Bessel function of the order of l. The spin states are not considered since they do not play any role in this study. Therefore, in Maxwell–Boltzmann statistics the single-particle partition function may be written as

$$\zeta = \sum_{m,l,n} \exp\left(-\frac{\varepsilon_{nlm}}{k_b T}\right) \tag{2a}$$

$$\zeta = \sum_{m=-l}^{l} \sum_{l=0}^{\infty} \sum_{n=1}^{\infty} \exp\left[-\left(\frac{\alpha x_{nl}}{\pi}\right)^2\right] = \sum_{l=0}^{\infty} (2l+1) \sum_{n=1}^{\infty} \exp\left[-\left(\frac{\alpha x_{nl}}{\pi}\right)^2\right], \tag{2b}$$

where k_b is Boltzmann's constant, T is the temperature and α is a dimensionless scale factor defined as $\alpha = h/(2\sqrt{2m_a k_b T}R) = L_c(T)/R$, $L_c(T)$ is one-half of the most probable de Broglie wavelength of the particles at temperature T.

Exact value of the partition function in equation (2b) can be calculated numerically by use of the exact roots, which in turn also need to be determined numerically. However, the calculation time is inversely proportional to the value of α for the desired accuracy of the partition function. For helium-4 at 300 K L_c equals 0.045 nm. Therefore, the calculation
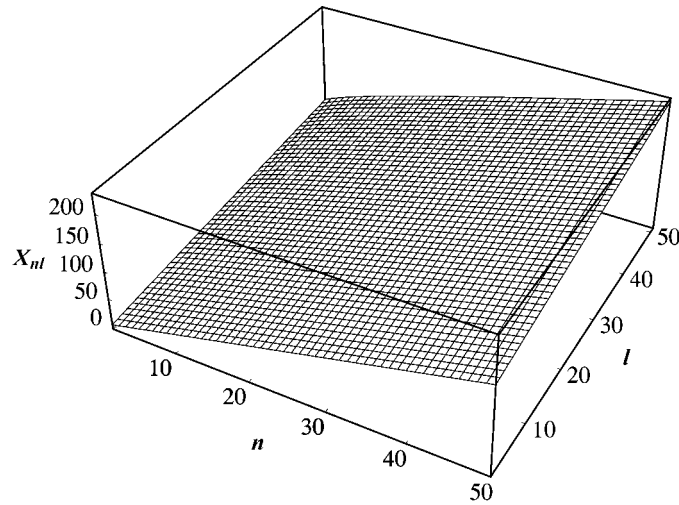
Figure 1. The nth root of the spherical Bessel function of the order of l versus n and l.

time becomes longer when the radius of the domain increases. The calculation process to be unpractical for a sphere with radius $R \gg L_c$. Furthermore, to obtain an analytical result for the partition function, it is necessary to use an approximate function for the roots of spherical Bessel functions. Their exact values are given in figure 1 as a function of n and l. It is seen that the roots essentially lie on a flat surface which may be approximated by

$$x_{nl} = c_n n + c_l l. \tag{3}$$

The values of c_n and c_l are determined numerically by equalizing the partition function based on equation (3) to the one with the exact roots.

The usual way to calculate the summations in equation (2b) is to use the integral approximation and replace the sums by integrals. For large systems the result of the integral approximation deviates only negligibly from the result of the summations. Such small deviations, however, become noticeable for systems on the micron or sub-micron scale. An exact way to calculate the sums is by use of the Poisson summation formula [23], which for a symmetric function may be expressed as

$$f(i) = f(i) \quad \Rightarrow \quad \sum_{i=1}^{\infty} f(i) = \int_0^{\infty} f(i)\, \mathrm{d}i - \frac{f(0)}{2} + 2 \sum_{s=1}^{\infty} \int_0^{\infty} f(i) \cos(2\pi s i)\, \mathrm{d}i. \tag{4}$$

The first term on the right-hand side is the dominant and conventional integral term. The second one is the zero correction term, which excludes the false contribution of the zero value of i to the integral term. The third one is the discreteness correction due to discrete values of i instead of continuous ones. It is possible to show numerically that the discreteness correction is much smaller than the zero correction as long as the system size is bigger than L_c ($\alpha < 1$). As an example, the ratio of the discreteness correction to the zero correction for the summation over n in equation (2b) for $l = 0$ is in the order of 1.8×10^{-4} even for α as large as unity. Therefore, the main correction to the integral approximation comes from the second term in equation (4) for small values of α.

The symmetry property of the function $\exp[-(\alpha x_{nl}/\pi)^2]$ in equation (2b) permits the use of equation (4). From the first two terms in equation (4) and by use of equation (3) the single-particle partition function (equation (2b)) is determined as

$$\zeta = \frac{\pi^{7/2}}{4\alpha^3 c_n c_l^2} \left[1 - \frac{2\alpha}{\pi^{3/2}}(c_n - c_l) - \frac{\alpha^2}{\pi^2}c_l(c_n - c_l) - \frac{\alpha^3 c_n c_l^2}{\pi^{7/2}} \right]. \tag{5}$$

It is known that the leading term in equation (5), $\pi^{7/2}/4\alpha^3 c_n c_l^2$, provides the conventional thermodynamic properties. Therefore, it must be independent of geometry. This quantity can be written as $3\pi^{5/2}V/16L_c^3 c_n c_l^2$ in term of volume V by elimition of α. For a rectangular geometry the leading term is $\pi^{3/2}V/8L_c^3$ [22]. Both equations must be equal and therefore we must have $c_n c_l^2 = 3\pi/2$. By use of this relation, and of half a million exact roots of the spherical Bessel functions, the approximate partition function and the exact one can be shown to agree if $c_n \to 3.514$ and $c_l \to 1.158$ when α takes values much smaller than unity. Even for $\alpha = 0.01$, the error of the partition function in equation (5)—and with $c_n = 3.514$ and $c_l = 1.158$—is about 0.008% and this value decreases with a decreasing value of α, i.e., increasing radius. Therefore, it is possible to use equation (5) as an analytical expression for the partition function in the case of $\alpha < 0.01$ which is the interesting case here.

Because small values of α are considered here, the second- and third-order terms in the bracket given in equation (5) may be neglected. By use of $c_n = 3.514$ and $c_l = 1.158$ equation (5) becomes

$$\zeta = \frac{\pi^{5/2}}{6\alpha^3} \left[1 - \frac{3\alpha}{2\sqrt{\pi}} \right] = \frac{\pi^{3/2}V}{8L_c(T)^3} \left[1 - \frac{3}{2\sqrt{\pi}}\frac{L_c(T)}{R} \right], \tag{6}$$

where V is the volume of a sphere. For $\alpha = 0.01$, the contribution of the second term in equation (6) is approximately 100 times bigger than the error due to the approximation by equation (3). This ratio increases with decreasing values of α. Therefore, equation (6) can safely be used for $\alpha < 0.01$.

2.2. Existence of an unavoidable quantum surface free energy

The partition function of a gas of N atoms is given by $Z = \zeta^N/N!$. From $F = -k_bT \ln Z$, the free energy of the gas is obtained by use of the Stirling approximation and of $\ln(1 + x) \cong x$ for $x \ll 1$ as

$$F = -Nk_bT \left[\ln\left(\frac{CT^{3/2}}{n}\right) + 1 \right] + Nk_bT \frac{3}{2\sqrt{\pi}}\frac{L_c(T)}{R}, \tag{7}$$

where C abbreviates the $(2\pi m_a k_b)^{3/2}/h^3$. The first term is the conventional bulk-free energy of a spinless monatomic ideal gas obtained by the integral approximation, the first term in equation (4). The second term in equation (7) is a correction due to the second term in equation (4) and it represents the effect of surface modes on free energy. It is possible to re-write equation (7) in the following form:

$$F = F_V + F_A = Vf_V(n, T) + Af_A(n, T), \tag{8a}$$

where F_V is the bulk-free energy, $F_A = Af_A(n, T)$ is the quantum surface free energy, $n = N/V$ is the volumetric density of particles, $V = 4\pi R^3/3$ is the volume in which the gas is confined, $A = 4\pi R^2$ is the surface area of this volume, f_V and f_A are bulk and quantum

surface free energy densities defined, respectively, as

$$f_V(n, T) = \frac{F_V}{V} = -nk_bT\left[\ln\left(\frac{CT^{3/2}}{n}\right) + 1\right], \tag{8b}$$

$$f_A(n, T) = \frac{F_A}{A} = nk_bT\frac{L_c(T)}{2\sqrt{\pi}}. \tag{8c}$$

It is clear that $F_A = Af_A(n, T)$ is not a homogeneous function of order 1 on N and V. In other words, if we double the volume and number of particles by keeping the density and temperature constant, F_A does not increase twice since the increment in surface area is different than the increment in volume. This fact makes F a non-extensive free energy.

Due to the wave character of atoms, F_A is an unavoidable component of the free energy and it is independent of the molecular interactions but depends on the geometric property of the domain, namely A/V. On the other hand, F_A is proportional to the quantity of $L_c(T)A/V$ which becomes negligible for large systems since $L_c(T)$ is also a very small quantity for ordinary temperatures. Therefore, the contribution of F_A to the free energy is noticeable only for microsystems.

2.3. Other thermodynamics properties

Pressure, chemical potential, entropy and energy are derived from the free energy by differentiation as

$$p = -\frac{1}{4\pi R^2}\frac{\partial F}{\partial R} = nk_bT + nk_bT\frac{1}{2\sqrt{\pi}}\frac{L_c(T)}{R} = nk_bT + \frac{f_A(n, T)}{R}, \tag{9}$$

$$\mu = \frac{\partial F}{\partial N} = -k_bT\ln\left(\frac{CT^{3/2}}{n}\right) + k_bT\frac{3}{2\sqrt{\pi}}\frac{L_c(T)}{R}, \tag{10}$$

$$S = -\frac{\partial F}{\partial T} = Nk_b\left[\ln\left(\frac{CT^{3/2}}{n}\right) + \frac{5}{2}\right] - \frac{Nk_b}{2}\frac{3}{2\sqrt{\pi}}\frac{L_c(T)}{R}, \tag{11}$$

$$E = F + TS = \frac{3}{2}Nk_bT + \frac{Nk_bT}{2}\frac{3}{2\sqrt{\pi}}\frac{L_c(T)}{R}. \tag{12}$$

In these equations, the first terms are the conventional terms and the second ones are the correction terms. The latter ones may be identified by the occurrence of L_c. For He-4 gas at 300 K and 10^5 Pa ($\approx$1 atm), $f_A(n, T)$ in equation (9) equals approximately $10^{-6}\,\mathrm{N\,m^{-1}}$ and it gives 1 Pa pressure correction for a system with 1 μm radius. At this point, it is worth noting that correction terms are not directly related with the ground-state energy of the particles, which is second order in $L_c(T)/R$.

The correction term in equation (10) shows that the chemical potential of a gas confined in a small sphere is bigger than that of the same gas confined in a large sphere even if both have the same density and temperature. This leads to diffusion between small and large systems because of the size difference. This kind of diffusion has been exhibited in [22] for a rectangular geometry. Furthermore, by use of equations (7), (9) and (10), it is seen that Gibbs free energy per particle is not equal to chemical potential even for spherical geometry, where the pressure is isotropic.

3. Thermodynamic properties in a cylindrical geometry

Thermodynamic properties of a monatomic ideal gas confined in a cylindrical geometry may be calculated by following the same method as in the previous section. The solution of the Schrödinger equation gives the following energy eigenvalues

$$\varepsilon_{nlk} = \frac{\hbar^2}{2m_a}\left[\left(\frac{x_{nl}}{R}\right)^2 + \left(\frac{\pi}{H}k\right)^2\right] \qquad \text{with} \quad \begin{array}{l} n = 1, 2, 3, \ldots \\ l = -\infty, \ldots, -1, 0, 1, \ldots, \infty, \\ k = 1, 2, 3, \ldots \end{array} \tag{13}$$

where R and H are the radius and the height of the cylindrical vessel, and x_{nl} is now the nth root of the ordinary Bessel function of order of l. Therefore, the single-particle partition function is written as

$$\zeta = \sum_{k=1}^{\infty}\sum_{l=-\infty}^{\infty}\sum_{n=1}^{\infty}\exp\left[-\left(\frac{\alpha_R x_{nl}}{\pi}\right)^2 - (\alpha_H k)^2\right] \tag{14}$$

where α_R and α_H are dimensionless scale factors defined as $\alpha_R = L_c(T)/R$ and $\alpha_H = L_c(T)/H$ with $L_c(T) = h/(2\sqrt{2m_a k_b T})$. By use of the symmetry property of the function $\exp[-(\alpha_R x_{nl}/\pi)^2]$ equation (14) may be written as

$$\zeta = \sum_{k=1}^{\infty}\exp[-(\alpha_H k)^2]\left[2\sum_{l=1}^{\infty}\sum_{n=1}^{\infty}\exp\left[-\left(\frac{\alpha_R x_{nl}}{\pi}\right)^2\right] + \sum_{n=1}^{\infty}\exp\left[-\left(\frac{\alpha_R x_{n0}}{\pi}\right)^2\right]\right] \tag{15}$$

which permits the use of equation (4). Similar to the roots of spherical Bessel functions, the roots of ordinary Bessel functions also essentially lie on a flat surface, which can be represented by equation (3). By using first and second terms in equation (4) and considering equation (3) for x_{nl}, the single-particle partition function is obtained as

$$\zeta = \frac{\pi^{5/2}}{2\alpha_R^2 \alpha_H c_n c_l}\left[1 - \frac{1}{\sqrt{\pi}}\left(\frac{c_n \alpha_R}{2} + \alpha_H\right)\right]. \tag{16}$$

The required geometric independence of the leading term in equation (16) dictates that $c_n c_l = 4$ holds. By use of this relation the approximate partition function, based on equation (3), and the one calculated numerically from the exact roots of Bessel functions are found to be equal for $c_n \to 2$ and $c_l \to 2$ when α_R and α_H are much smaller than unity. By use of these values in equation (16) the single-particle partition function is obtained as

$$\zeta = \frac{\pi^{5/2}}{8\alpha_R^2 \alpha_H}\left[1 - \frac{1}{\sqrt{\pi}}(\alpha_R + \alpha_H)\right] = \frac{\pi^{3/2}V}{8L_c^3}\left[1 - \frac{L_c(T)}{\sqrt{\pi}}\left(\frac{1}{R} + \frac{1}{H}\right)\right]. \tag{17}$$

Thermodynamic properties are calculated by using equation (17) in a similar way as in section 2. Therefore, we may write

$$F = -Nk_b T\left[\ln\left(\frac{CT^{3/2}}{n}\right) + 1\right] + Nk_b T\frac{L_c(T)}{\sqrt{\pi}}\left(\frac{1}{R} + \frac{1}{H}\right), \tag{18a}$$

$$F = F_V + F_A = Vf_V(n, T) + Af_A(n, T), \tag{18b}$$

where F_V is the bulk (conventional) free energy, F_A is the quantum surface free energy, $V = \pi R^2 H$ is the volume in which the gas is confined, $A = 2\pi RH + 2\pi R^2$ is the surface area of this volume, f_V and f_A are the same given in equations (8b) and (8c), respectively.

Pressures in radial and axial directions are obtained as

$$p_R = -\frac{1}{2\pi RH} \frac{\partial F}{\partial R} = nk_b T + \frac{f_A(n, T)}{R},$$ (19a)

$$p_H = -\frac{1}{\pi R^2} \frac{\partial F}{\partial H} = nk_b T + \frac{2 f_A(n, T)}{H}.$$ (19b)

It is seen that the pressure tensor becomes anisotropic in cylindrical geometry. Chemical potential, entropy and energy are given as

$$\mu = -k_b T \ln\left(\frac{CT^{3/2}}{n}\right) + k_b T \frac{L_c(T)}{\sqrt{\pi}} \left(\frac{1}{R} + \frac{1}{H}\right),$$ (20)

$$S = Nk_b \left[\ln\left(\frac{CT^{3/2}}{n}\right) + \frac{5}{2}\right] - \frac{Nk_b}{2} \frac{L_c(T)}{\sqrt{\pi}} \left(\frac{1}{R} + \frac{1}{H}\right),$$ (21)

$$E = \frac{3}{2}Nk_b T + \frac{Nk_b T}{2} \frac{L_c(T)}{\sqrt{\pi}} \left(\frac{1}{R} + \frac{1}{H}\right).$$ (22)

4. Conclusion: geometry and size dependence of thermodynamics

By use of the equations (7) and (18a) and [22], free energy expressions in spherical, cylindrical and rectangular geometries are re-written, respectively as

$$F_{\text{sph}} = -Nk_b T \left[\ln\left(\frac{CT^{3/2}}{n}\right) + 1\right] + Nk_b T \frac{L_c(T)}{\sqrt{\pi}} \frac{3}{2R},$$ (23)

$$F_{\text{cyl}} = -Nk_b T \left[\ln\left(\frac{CT^{3/2}}{n}\right) + 1\right] + Nk_b T \frac{L_c(T)}{\sqrt{\pi}} \left(\frac{1}{R} + \frac{1}{H}\right),$$ (24)

$$F_{\text{rct}} = -Nk_b T \left[\ln\left(\frac{CT^{3/2}}{n}\right) + 1\right] + Nk_b T \frac{L_c(T)}{\sqrt{\pi}} \left(\frac{1}{L_x} + \frac{1}{L_y} + \frac{1}{L_z}\right),$$ (25)

where L_x, L_y and L_z are the dimensions of the rectangular box. From equations (23)–(25), it is seen that the correction terms are different for different geometries and we may summarize them in a single formula by using the ratio of surface area, A, to volume, V. Thus, free energy can be expressed as

$$F = -Nk_b T \left[\ln\left(\frac{CT^{3/2}}{n}\right) + 1\right] + Nk_b T \frac{L_c(T)}{2\sqrt{\pi}} \frac{A}{V}.$$ (26)

The second term in equation (26) is the general form of quantum surface free energy. Consequently, it is possible to say that the thermodynamic state functions of an ideal gas do not depend on only two variables, like temperature and density, but also depend on A/V, which depends on geometry and size. In other words, specific thermodynamic properties of two systems filled by the same gas at the same temperature and density are different, if their confinement geometries and/or sizes are different. Geometry and size differences become driving forces for diffusion, and geometric asymmetry causes pressure anisotropy. As a result, thermodynamics becomes non-extensive because it depends on A/V in general. Non-extensive thermodynamics is a branch of thermodynamics for systems having long-range interactions, like gravitational or unscreened coulomb interactions [24, 25]. However, it is seen

that even the thermodynamics of an ideal gas is non-extensive due to unavoidable existence of quantum surface free energy.

In a classical gas, which is represented by Maxwell–Boltzmann statistics, the number of particles in surface modes is always less than those in a Bose gas and more than those in a Fermi gas. Therefore, it is expected that the size effects considered here become stronger in a Bose gas while they become weaker in a Fermi gas. However, Bose–Einstein condensation makes the problem more complicate in the case of a Bose gas. Casimir-like size effects in ideal quantum gases are under consideration now. In a real gas confined in a finite domain, interactions between the particles give rise the classical surface free energy, which may become dominant and suppress the quantum one if the interaction potential is strong, gas density is high and the molecular mass is big (L_c is small). Helium gas has a small atomic mass and very weak interatomic interaction potential. Therefore, helium gas at low density is the best candidate to observe the surface dependency in thermodynamics of a classical gas confined in a micron or sub-micron scale.

For a given volume and temperature, the stable geometry of a system having a flexible surface is a sphere since the free energy is minimal in the spherical case. By considering the quantum surface free energy, it may be expected that an ideal gas in a paralloidal box may have shear stresses, which act on the surfaces of the box trying to transform it to a rectangular box, because the later one has less surface area than the paralloidal one for a given volume.

Acknowledgments

References

[1] Casimir H B G 1948 *Proc. Koninkl. Nederl. Akad. Wetenschap* **51** 793–6
[2] Milton K A 2001 *The Casimir Effect: Physical Manifestations of Zero-Point Energy* (New Jersey: World Scientific)
[3] Mostepanenko V M and Trunov N N 1997 *The Casimir Effect and Its Applications* (Oxford: Clarendon)
[4] Bordag M, Mohideen U and Mostepanenko V M 2001 *Phys. Rep.* **353** 1–205
[5] Reith M 2003 *Nano-Engineering in Science and Technology* (NJ: World Scientific)
[6] Timp G 1999 *Nanotechnology* (New York: Springer)
[7] Chan H B, Aksyuk V A, Kleiman R N, Bishop D J and Capasso F 2001 *Phys. Rev. Lett.* **87** 211801, 1–4
[8] Buks E and Roukes M L 2001 *Eur. Phys. Lett.* **54** 220–6
[9] Buks E and Roukes M L 2001 *Phys. Rev.* B **63** 033402, 1–4
[10] Serry F M, Walliser D and Maclay G J 1998 *J. Appl. Phys.* **84** 2501–6
[11] Esquivel-Sirvent R, Villarreal C, Mochan W L and Cocoletzi G H 2002 *Phys. Status Solidi* b **230** 409–13
[12] Pinto F 1999 *Phys. Rev.* B **60** 740–55
[13] Sisman A and Saygin H 2001 *Proc. Second Int. Heat Powered Cycle Conf. (Paris, France, 5–7 September 2001)* pp 147–51
[14] Ambjorn J and Wolfram S 1983 *Ann. Phys.* **147** 1–32
[15] Revzen M, Opher R, Opher M and Mann A 1997 *J. Phys. A: Math. Gen.* **30** 7783–9
[16] Mitter H and Robaschik D 2000 *Eur. Phys. J.* B **13** 335–40
[17] Feinberg J, Mann A and Revzen M 2001 *Ann. Phys., NY* **288** 103–36
[18] Bezerra V B, Klimchitskaya G L and Mostepanenko V M 2002 *Phys. Rev.* A **66** 062112, 1–13
[19] Bezerra V B, Klimchitskaya G L and Mostepanenko V M 2002 *Phys. Rev.* A **65** 052113, 1–7

[20] Bordag M, Nesterenko V V and Pirozhenko I G 2002 *Phys. Rev.* D **65** 045011, 1–16
[21] Larraza B and Denardo B 1998 *Phys. Lett.* A **248** 151
[22] Sisman A and Müller I 2004 *Phys. Lett.* A **320** 360–6
[23] Murray R S 1968 *Mathematical Handbook of Formulas and Tables* (New York: McGraw-Hill) p 109
[24] Kaniadakis G, Lissia M and Rapisarda A 2002 *Physica* A **305** 1
[25] Tsallis C 2002 *Chaos Solitons Fractals* **13** 371